Journal of Physics: Conference Series

PAPER • OPEN ACCESS

Feasibility study of the employment of laser Doppler Vibrometry for photoacoustic imaging

IOP Conf. Series: Journal of Physics: Conf. Series 1149 (2018) 012028 doi:10.1088/1742-6596/1149/1/012028

Feasibility study of the employment of laser Doppler Vibrometry for photoacoustic imaging

L Mignanelli[1] and C Rembe

Clausthal University of Technology,Leibnizstraße 28, Clausthal-Zellerfeld, Germany

[1]mignanelli@iei.tu-clausthal.de

Abstract. Photoacoustic imaging (PAI) is a biomedical imaging method which seems very promising for the detection of tumors in breast or in brain. Currently the detection of these signals is performed with piezoelectric transducers, which are very sensitive but have several limitations. Laser Doppler Vibrometry (LDV) represents a good alternative because it is a noncontact technique. The purpose of this paper is to investigate the potentiality of LDV for PAI in comparison with current transducers, and understand, in which measuring condition it is reasonable to adopt it. First, we make an introduction about the theory of PAI, we present a model of PAI for LDV and then, we investigate the theoretical limits for PAI with LDV. We derive a minimal detectable tumour radius of 390 µm for a commercial LDV with He-Ne laser.

1. Introduction

Photoacoustic imaging (PAI) is an imaging technique based on the photoacoustic effect. The main applications of PAI are in imaging of molecules, microvasculature, tumors, brain, and small animals [1-3]. This technique provides the use of a short-pulse light source for the irradiation of the tissue, this leads to the generation of a broadband photoacoustic (PA) wave. The PA wave propagates through the tissue and it is detected with ultrasound (US) transducers, and an image is computed.

The ultrasound transducers used for PAI present a high sensitivity but they have limitations due to the narrow frequency bandwidth, the finite aperture size, the contact nature of the device and the need of a coupling medium [4]. Optical detection of ultrasound could represent a valid alternative, thus several research groups investigated different interferometric techniques for PA applications [4-7]. In particular reference [4] presents a study of an all-optical non-contact PAI by using a commercial laser Doppler vibrometer (LDV) [8]. In reference [4] the authors present experiments on a pig brain with an artificial tumor as absorbing object, showing that LDV offers a promising method to achieve a non–contact PAI.

In this work, we investigated for which conditions it is reasonable to use LDV for PAI. We investigated which are the limits of detection for LDV depending on the metrological characteristics of the device and on the geometry of the investigated object. We introduce at first the typical signals generated from a spherical absorbing object and we examined the suitability of the LDV in comparison with ultrasonic transducers.

2. Photoacoustic imaging theory

Photoacoustic imaging is based on the photoacoustic effect. A short laser pulse irradiates the tissue, the light is locally absorbed, and converted into heat. The temperature rise of the irradiated object induces a pressure rise through thermoelastic expansion. This process is widely described in [1-3,9-14]. In particular the fractional volume expansion of the heated region is

$$\frac{\mathrm{d}V}{V} = -\kappa p + \beta T, \tag{1}$$

κ is the isothermal compressibility, β is the coefficient of volume expansion, and T is the change in temperature. Neglecting volume expansions, $\mathrm{d}V/V = 0$ during the fast heating, i.e. assuming that the laser pulse is shorter than the thermal and stress relaxation times, [1-3] the initial pressure can be calculated as

$$p_0 = \frac{\beta T}{\kappa} = \frac{\beta A_\mathrm{e}}{\kappa \rho C_\mathrm{V}} = \Gamma A_\mathrm{e}. \tag{2}$$

The temperature increase T can be expressed as the specific optical energy deposition A_e divided by the density of the material ρ and the heat capacity at constant volume C_V. $\Gamma = \beta / \kappa \rho C_V$ is the Grüneisen parameter. If all absorbed energy is converted into heat [3], A_e can be expressed as the optical fluence F of the laser beam multiplied by the optical absorption coefficient μ_a

$$p_0 = \Gamma \mu_\mathrm{a} F. \tag{3}$$

The originated pressure propagates as an ultrasound wave in the tissue according with the wave equation

$$\left(\nabla^2 - \frac{1}{v_\mathrm{s}} \frac{\partial^2}{\partial t^2}\right) p(\boldsymbol{r}, t) = -\frac{\beta}{\kappa v_\mathrm{s}^2} \frac{\partial^2 T(\boldsymbol{r}, t)}{\partial t^2}, \tag{4}$$

where v_s is the sound velocity in the material and $p(\boldsymbol{r}, t)$ is the pressure at the location $\boldsymbol{r}$ and time instant t. Equation (4) can be solved with the Green's function approach, as the response to a temporal and spatial impulse [1-3] leading to

$$p(\boldsymbol{r}, t) = \frac{1}{4\pi v_\mathrm{s}^2} \frac{\partial}{\partial t} \left[\frac{1}{v_\mathrm{s} t} \int d\boldsymbol{r}' p_0(\boldsymbol{r}') \delta\left(t - \frac{\boldsymbol{r} - \boldsymbol{r}'}{v_\mathrm{s}} \right) \right], \tag{5}$$

where δ is the delta function and $\boldsymbol{r}'$ is the position of the source location. This equation is expressed in spherical coordinates and it is valid to calculate the photoacoustic pressure generated by an arbitrary heterogeneous optically absorbing object heated by a short laser pulse in stress and thermal confinement conditions. A detailed description of the mathematics can be found in [1-3].

2.1. Typical photoacoustic signal generated from a spherical absorbing object

Equation (6) describes the pressure propagation of a homogeneously heated sphere which could represent an early stage tumor in breast tissue [9]. For the case of a small sphere, the pressure p at the time instant t and at the distance r from the center of the sphere (Figure 1) [1], can be derived from equation (5) by

$$p(r, t) = p_0 \left[U(R_S - v_\mathrm{s} t - r) + \frac{r - v_\mathrm{s} t}{2r} U\left(r - |R_S - v_\mathrm{s} t|\right) U(R_S + v_\mathrm{s} t - r) \right], \tag{6}$$

where U is the Heaviside function and R_S is the radius of the small sphere [1-3]. Therefore, the signal generated by a small sphere with higher absorption has a bipolar shape. The amplitude is inversely proportional to the distance r from the sphere/tumor and directly proportional to the initial pressure p_0. In particular, the duration τ of the bipolar signal depends on R_S

$$\tau = \frac{2R_S}{v_\mathrm{s}}. \tag{7}$$

Figure 1 shows the set-up for measurements performed in transmission, i.e. the transducer is positioned in the opposite side of the excitation at the distance r_d from the sphere. Figure 2 shows the signal generated by a small heated and expanded sphere with $R_S = 0.5$ mm acquired for different detector distances $(r = r_d)$ according with equation (6). Acoustic attenuation was not considered for this simulation. The duration of the signal τ remains the same since R_S and v_s are fixed, but the amplitude is damped by a factor $1/2r$.

The amplitude of the positive peak of the bipolar signal when the photoacoustic wave reaches the detector position r_d is [9-11]

$$p_{peak}(r_d) = \frac{1}{2r_d} \Gamma \mu_\mathrm{a} F(z_S) R_S, \tag{8}$$

where $F(z_S)$ is the laser fluence at the position of the object (z_S), F_0 is the fluence on the surface and μ_{eff} is the effective optical attenuation in the tissue

$$F(z_S) = F_0 e^{(-\mu_{\text{eff}} z_S)}. \tag{9}$$

The acoustic attenuation of the wave travelling through a medium plays an important role in ultrasound imaging. Soft tissue has a typical acoustic attenuation coefficient [2, 10]

$$\mu_{\text{ac}}(f) = 0.1\left[\frac{\text{dB}}{\text{cm MHz}}\right] f_{(\text{MHz})}, \tag{10}$$

where $f_{(\text{MHz})}$ is the frequency of the signal in MHz. Equation

$$p_{peak}(r_d) = \frac{1}{2r_d}\Gamma\mu_{\text{a}}F(z_S)R_S \cdot \exp(-\mu_{\text{ac}}(f)r_d) \tag{11}$$

includes also the acoustic attenuation through the tissue by multiplying equation (8) with the damping. The frequency spectrum of the bipolar signal presents a characteristic sequence of oscillations which decrease in amplitude. In particular the central frequency f_{u} depends on the sound velocity and the dimension of the object [10-12]

$$f_u = 0.33\frac{v_{\text{s}}}{R_S}. \tag{12}$$

The major portion of acoustic energy resides in the half-power bandwidth (-3dB), i.e. between $f_{\text{low,-3dB}} = 0.16 v_{\text{s}} / R_S$ and $f_{\text{upper,-3dB}} = 0.51 v_{\text{s}} / R_S$ [2,10-12]. If we take for example, $R_S = 1$ cm, $r_d = 2$ cm and $v_{\text{s}} = 1545$ m/s, the attenuation factor $\exp(-\mu_{\text{ac}}(f)\cdot r_d)$ at $f = f_{\text{u}}$ results in $\exp(-\mu_{\text{ac}}(f_{\text{u}})\cdot r_d) = 0.9899$, at $f = f_{\text{low,-3dB}}$ and $f = f_{\text{upper,-3dB}}$ is $\exp(-\mu_{\text{ac}}(f_{\text{low,-3dB}})\cdot r_d) = 0.9951$ and $\exp(-\mu_{\text{ac}}(f_{\text{upper,-3dB}})\cdot r_d) = 0.9844$ respectively. The error of the attenuation factor by considering f_{u} instead of the frequencies inside the half power bandwidth is : 1% in this example. In this first essay we assume the attenuation factor $\exp(-\mu_{\text{ac}}(f_{\text{u}})\cdot r_d)$ not only for the central frequency but for the whole spectrum of the pulse. Thus, the frequency dependence is only considered for the center frequency of the signal in our model.

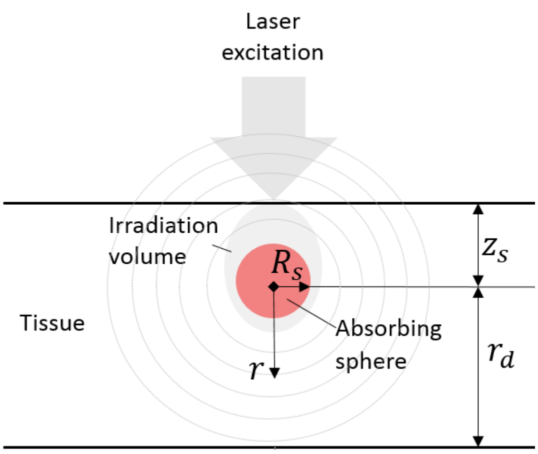

Figure 1. Setup for photoacoustic measurement performed in transmission. The acquisition sensor is positioned at r_d [9]

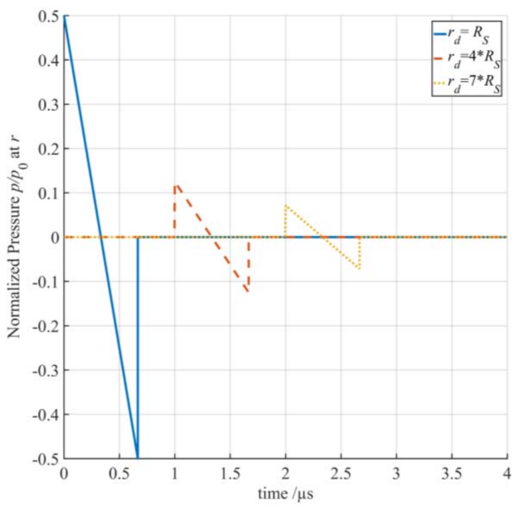

Figure 2. Simulation of the signal generate by a small sphere with $R_S = 0.5$ mm [1-3] at different distances r_d

3. Photoacoustic signal detection with LDV

The LDV is a noncontact interferometric technique that employs a heterodyne detection scheme [8]. It allow the detection of real time velocity and displacement signals with a resolution down to picometer range. An LDV sensor measures the Doppler shift of the back-scattered measurement beam which impinges the moving object. Reference [8] provides a detailed description of the measurement principle. LDV sensors are widely used for noncontact surface vibration measurements in mechanical, civil and industrial engineering. Due to its metrological properties and its non-contact nature, this technique finds also several application in the biomedical field like the identification of the cardiovascular parameter, studies of the ear, and dentistry. Recently LDV was employed for PA detection [4].

3.1. Measurement condition for the detection of PAI signals with LDV

Photoacoustic detectors are usually broadband ultrasound sensor, here we present the measurement condition for the alternative solution with a LDV proposed in reference [4]. While ultrasound sensors measure the pressure, LDV sensors measure the velocity or the displacement. In order to be able to detect the PA signal without degradation, two main conditions need to be fulfilled:

a) The maximal detectable frequency of the sensor has to be greater than the characteristic frequencies of the photoacoustic signals, which are strictly related to the minimal dimension of the absorbing object. According with [2], to acquire PA signals properly a bandwidth of 150% in respect to the central frequency f_{u} is necessary

$$\%B = \frac{f_{\mathrm{H}} - f_{\mathrm{L}}}{f_{\mathrm{u}}}. \tag{13}$$

This represent a good compromise between the detection of high frequency components and the noise level. The typical bandwidth of LDV has a lower frequency f_{L}=0 Hz and an upper frequency of f_{H}=2 MHz [8]. The minimal detectable absorbing object is calculated by combining equation (12) and (13).

b) The pressure, the velocity or the displacement at the boundary needs to be larger than the resolution of the sensor. In the case of the LDV the minimal detectable velocity or the minimal detectable displacement has to be greater than the velocity/displacement at the boundary.

The minimal detectable displacement of a heterodyne interferometer is related to the signal to noise ratio referred to 1 Hz bandwidth (SNR'). In particular the noise equivalent mean square displacement d'_{min} after demodulation [8] is

$$d'_{\mathrm{min}} = \frac{\lambda}{4\pi}\left(SNR'\right)^{-1/2}, \tag{14}$$

λ is the wavelength of the laser source. In theoretic calculations d'_{min} can reach $4\ \mathrm{fm}\cdot\mathrm{Hz}^{-1/2}$ [8]. However, commercially available class II LDVs are in combination with digital decoding that yields to a resolution of about $d'_{\mathrm{min}} = 50\ \mathrm{fm}\cdot\mathrm{Hz}^{-1/2}$ [8]. Thus we made the assumption that the displacement resolution of LDV at a given bandwidth B, $d_{\mathrm{min}@B}$, can be expressed in terms of power spectral density (PSD) of a white noise

$$d_{\mathrm{min}@B} = \left(\int_{\nu_1}^{\nu_2=\nu_1+B} PSD(\nu)\,d\nu\right)^{1/2} = d'_{\mathrm{min}}\cdot(B)^{1/2}, \tag{15}$$

where ν_1 and ν_2 are respectively the lower and the upper frequencies of the bandwidth. As mentioned before, the typical bandwidth of commercial LDV is 0-2 MHz, thus

$$d_{\mathrm{min}@B=2\mathrm{MHz}} = 50\frac{\mathrm{fm}}{\mathrm{Hz}^{1/2}}\cdot\left(2\ \mathrm{MH}z\right)^{1/2} = 70.7\ \mathrm{pm}. \tag{16}$$

We investigate for which combination of parameters (R_S, r_d, z_S) and metrological characteristics $(B, d_{\mathrm{min}@B})$ the detection with LDV is feasible.

4. Discussion

4.1. Resolution comparison between US sensors and LDV

An important aspect is to understand when it is reasonable to apply the LDV for PA detection in comparison with US sensors. While the typical resolution for commercial LDV is $d'_{\mathrm{min}} = 50\ \mathrm{fm}\cdot\mathrm{Hz}^{-1/2}$, the typical resolution for broadband ultrasound sensors is in the range of $0.2\text{-}0.6\ \mathrm{mPa}\cdot\mathrm{Hz}^{-1/2}$ [12]. The pressure resolution p'_{min} can be expressed in displacement resolution $d_{\mathrm{min,p}}$ in $\mathrm{m}\cdot\mathrm{Hz}^{-1/2}$ and compared with the LDV one, by considering the resolution for a sinusoid with frequency f at the boundary skin/air [13]

$$p'_{\mathrm{min}} = \frac{Z}{2} 2\pi f d'_{\mathrm{min,p}} \Rightarrow d'_{\mathrm{min,p}} = \frac{p'_{\mathrm{min}}}{Z\pi f}. \tag{17}$$

where Z is the acoustic impedance of the tissue. The factor 2 depends on the impedance mismatch between skin and air which results in an asymmetric displacement in direction of the skin-air interface [14].

In figure 3 the resolution of the different sensors are compared. In particular the resolution of a broadband ultrasound sensor ($0.6\ \mathrm{mPa}\cdot\mathrm{Hz}^{-1/2}$) and of a commercial class II He-Ne LDV are reported. In addition, since the newest LDVs have an infrared (IR) laser(1550 nm) and this technology seem very promising, we show in figure 4 also the theoretical resolution limit for a 1550 nm heterodyne interferometer $d'_{\mathrm{min,IR}}=0.88\ \mathrm{fm}\cdot\mathrm{Hz}^{-1/2}$ [4].

Figure 3 reveals that for frequencies lower than ~1 kHz the commercial LDV has better resolution than broadband US transducers. This limit can go theoretically up to almost 100 kHz with IR technology. Since typically the ultrasonic frequency spectrum of PA signals has components between 100 kHz-10 MHz [12], US transducers have generally better performances than LDV for the detection of PA signals. However the detection of PA signals with LDV is possible according to the conditions described in paragraph 3.1.

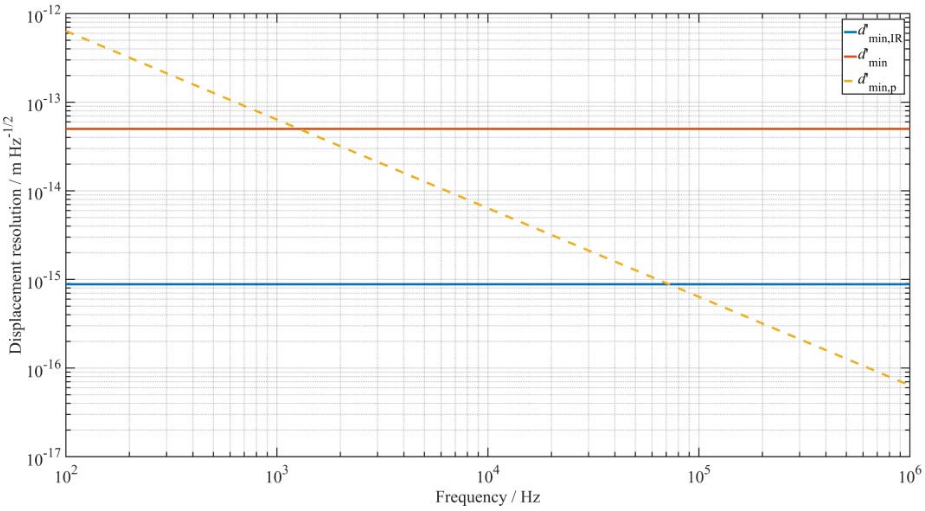

Figure 3. Comparison between the resolution of LDV and broad band US transducers

4.2. Limits of LDV for the detection of PA signals

According to the condition a) in paragraph 3.1, for a proper reconstruction of a PA signal with LDV, its central frequency has to be lower as $f_{\mathrm{u,max}}$

$$f_{\mathrm{u,max}} = \frac{100}{150}\cdot\left(f_{\mathrm{H}} - f_{\mathrm{L}}\right)=1.3\ \mathrm{MHz}. \tag{18}$$

From equation (12) it is possible to relate $f_{\mathrm{u,max}}$ to the corresponding dimension of the object $R_{S,\mathrm{min}}$ as

$$R_{S,\mathrm{min}} = 0.33\frac{v_s}{f_{\mathrm{u,max}}}, \tag{19}$$

with the assumption of $v_s = 1545$ m/s (typical sound velocity for soft tissue). The minimal detectable absorbing object with LDV is $R_{S,\mathrm{min}} = 0.39$ mm.

Conform to the second detection condition, $d_{\min@B}$ has to be lower than the maximal displacement amplitude at the boundary. At the boundary between skin and air at $r = r_d$ the relation, between pressure p and velocity v [13] is

$$v(r_d, t) = \frac{2 \cdot p(r_d, t)}{Z}. \tag{20}$$

The equation (20) can be expressed in terms of displacement d

$$d(r_d, t) = \int \frac{2 \cdot p(r_d, t)}{Z} dt . \tag{21}$$

The velocity signal is directly proportional to the pressure and thus, except for an amplitude factor, it has the same characteristics in time and in frequency domain of the pressure signal. The displacement signal is presented in figure 4. Its maximum amplitude is $d_{\max}$

$$d_{\max} = \frac{1}{2}\left(\frac{2 p_{peak}(r_d)}{Z} \cdot \frac{\tau}{2}\right). \tag{22}$$

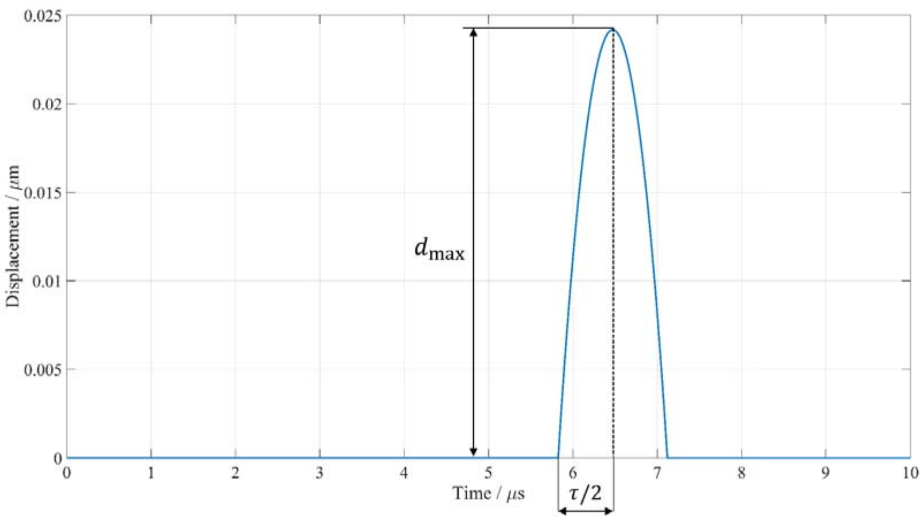

Figure 4. Example of a displacement signal $d(r_d, t)$ generated by $R_S = 1$ mm, $r_d = 1$ cm and $z_S = 1$ cm. The value of the other parameters are the same as in figure 5.

We calculate the value of $d_{\max}$ in dependence on all relevant parameters (R_S, r_d, z_S and μ_a) of the set up and the excitation. From (11) and (22) we have

$$d_{\max} = \frac{R_S}{Z \cdot v_s} \frac{1}{2 \cdot r_d} \Gamma \mu_a F(z_S) R_S \cdot \exp\left[-\mu_{ac}(f) r_d\right]. \tag{23}$$

In figure 5 we presented a map of $d_{\max}$ generated by an absorbing object with dimension $R_{S,\min} = 0.39$ mm in function of the depth z_S and the distance between the tumor and the acquisition system r_d. In particular we assumed $v_s = 1545$ m/s, $Z = 1.5$ MRayl, $\Gamma = 0.8$, $\mu_a = 0.6$ cm^{-1}, $\mu_{\text{eff}} = 1.2$ cm^{-1} and $\mu_{ac}(f_u)$ [9-11,14]. We chose a pulsed laser with 1064 nm wavelength as laser excitation. The maximal allowed laser fluence for application in human body according with the laser safety norm [15] is $F_0 = 100$ mJ cm^{-2}.

By comparing the value of $d_{\min@B=2\text{MHz}}$ with the values of $d_{\max}$ in figure 5 it is possible to notice that a sphere with a 0.39 mm radius and $\mu_a = 0.6$ cm^{-1} can be detected for the combination of z_S and r_d in the yellow range of the figure $\left(d_{\max} > d_{\min@B=2\text{MHz}} = 70.7 \text{ pm}\right)$. The interval is delimited by the distance to the detector $r_d < 16.5$ mm and the tumour-depth $z_S < 33.4$ mm.

We analysed also the maximal depth z_S where the simulated spheres with $R_{S,\min}$ are still detectable depending on the absorption coefficient μ_a for $z_S = r_d$. In figure 6 the results are displayed. With an absorption coefficient of $\mu_\mathrm{a} = 1\ \mathrm{cm}^{-1}$ (typical value for a tumor with 12% blood [14]) the maximal depth z_S where the signal generated by a sphere with $R_{S,\min}$ is still detectable (yellow range) is ~9.7 mm.

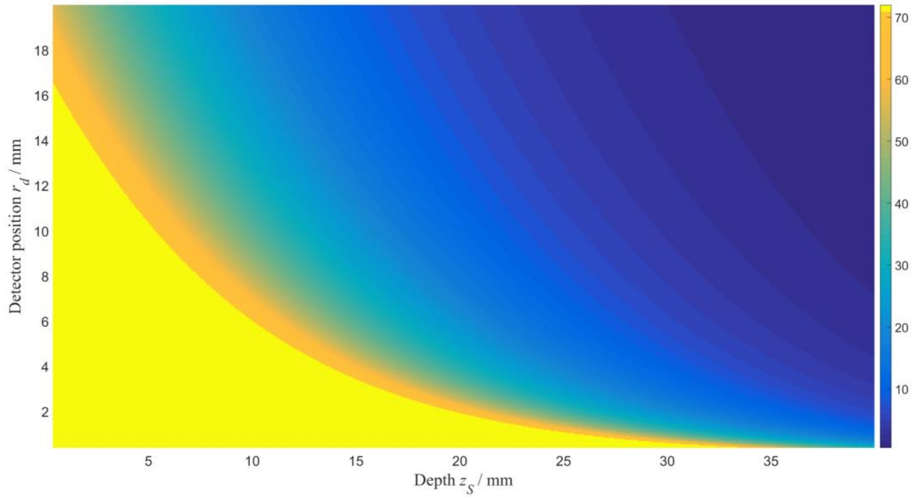

Figure 5. The colourmap presents the value of $d_{\max}$ in pm generated by a sphere with $R_{S,\min}$ in function of the depth z_S and the distance from the acquisition system r_d. The yellow range indicates where the sphere is detectable $\left(d_{\max} > d_{\min@B=2\mathrm{MHz}} = 70.7\ \mathrm{pm}\right)$.

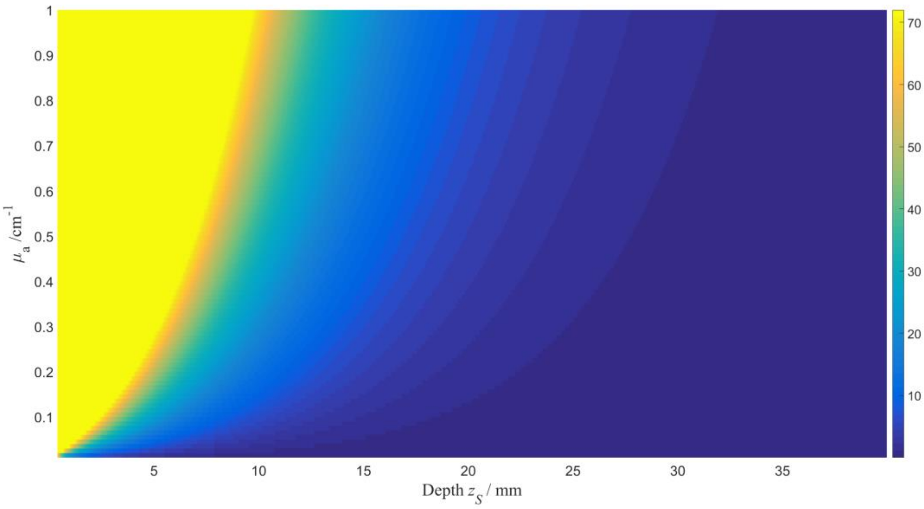

Figure 6. The colormap presents the value of $d_{\max}$ in pm generated by a sphere with $R_{S,\min}$ in function of the absorption coefficient μ_a and the depth z_S. The distance of the detector for this simulation is $r_d = z_S$. The yellow range indicates where the sphere is detectable.

Figure 7 shows a comparison between the minimal detectable displacement with the LDV and the maximal displacement $d_{\max}$ generated by a heated sphere. For the LDV minimal displacement we present three cases:

a) Commercial He-Ne LDV with $B = 2\ \mathrm{MHz}$, thus $d_{\min@B=2\mathrm{MHz}}$.

b) According with equation (13) for objects bigger than $R_{S,\min}$, the necessary detection bandwidth is smaller than 2 MHz. With a smaller bandwidth the noise level is lower, and thus, if possible, it is convenient to measure with a bandwidth $B(R_S)$

$$B(R_S) = \frac{150}{100} \cdot f_{\mathrm{u}} = \frac{150}{100} \cdot 0.33 \cdot \frac{v_s}{R_S}. \tag{24}$$

Therefore, we obtain a minimal displacement $d_{\min @ B(R_S)}$ that varies with the necessary bandwidth

$$d_{\min @ B(R_S)} = d'_{\min} \cdot \left(B(R_S)\right)^{1/2}. \tag{25}$$

c) The theoretical resolution limit of a 1550 nm heterodyne interferometer with the bandwidth varying with the radius of the sphere $B(R_S)$

The curves of case a), b) and c) are graphically, compared with the curves of $d_{\max}$ over the radius R_S at different depths z_S, $d_{\max}(z_S)$. In particular we chose $z_S = 1$ cm, $z_S = 2$ cm and $z_S = 3$ cm. The detector distance is fixed at $r_d = 1$ cm and the other parameters have the same values as the simulation performed in figure 5. Figure 7 allows to determine when a measurement with a commercial He-Ne LDV is feasible depending on the size of the absorbing object R_S. A measure is feasible if the value of the displacement originated from the heated sphere is, for a given R_S, above the displacement resolution limit of the LDV. In case b), due to the reduction of the bandwidth depending on R_S, the resolution increases allowing the detection of the same object at greater z_S respect to the case a). Case c) has always the highest resolution. For example, for a sphere with $R_S = 0.8$ mm placed at $z_S = 1$ cm, $d_{\max}(z_S = 1 \text{ cm})$ is detectable in all three cases. If the depth increases, $z_S = 2$ cm, only case b) and c) can detect $d_{\max}(z_S = 2 \text{ cm})$. The sphere at $d_{\max}(z_S = 3 \text{ cm})$ is detectable only in case c). Case c) presents the best measuring conditions and it can be considered the theoretical limited for the acquisition of PA signals with LDV.

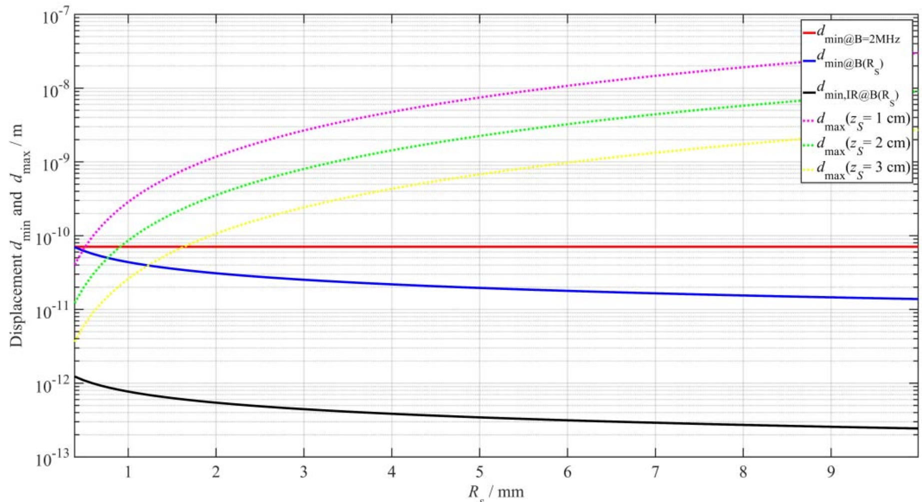

Figure 7. Comparison of the minimal detectable displacement with the maximal displacement originated by an absorbing sphere at different values of z_S. The three continuous lines represent the LDV minimal displacement calculated as described in case a), b) and c). The upper one is $d_{\min @ B=2\mathrm{MHz}}$, the middle one is $d_{\min @ B(R_S)}$ and the lower one is $d_{\min, IR @ B(R_S)}$. The three dotted lines represent the displacement $d_{\max}$ over the radius R_S at different values of z_S. Starting from the top we have respectively $d_{\max}(z_S = 1 \text{ cm})$, $d_{\max}(z_S = 2 \text{ cm})$ and $d_{\max}(z_S = 3 \text{ cm})$.

5. Conclusion

In this paper we present a model of PAI for LDV and the potential of LDV for PAI in comparison with current transducers. We explore the measuring conditions for a reasonable adoption of the LDV. In addition, we derived the theoretical limits for PAI with LDV. The analysis indicates that the commercial LDV has better resolution than broadband US transducer for frequencies lower then 1 kHz. This limit can go theoretically up to almost 100 kHz with IR technology. Since typically the ultrasonic frequency spectrum of PA signals are about between 100 kHz -10 MHz [2], US broadband transducers have generally better resolution than LDV for the detection of PA signals. However, since LDV presents advantages due to the non-contact nature of the technology and it has sufficient resolution to detect PA signals, it is still reasonable to use LDV for PAI acquisition. LDV allows the detection of absorbing spherical objects with a radius down to 0.39 mm, depending on its depth in the tissue, and the absorption coefficient at the excitation wavelength.

Future works are oriented on experimental tests to verify the theoretical limits described in this work. We would like also to include in our model the frequency dependent attenuation and evaluate its effects on the limits of LDV for the detection of PA signals.

References

[1] Wang L V and Wu H 2007 *Biomedical optics: principles and imaging* (New York: Wiley-Interscience
[2] Wang, L. V. (Ed.), Thompson, B. 2009 Photoacoustic Imaging and Spectroscopy. (Boca Raton: CRC Press)
[3] Wang L V 2008 *IEEE J. Sel. Top. Quantum Electron* **14** 171
[4] Tian C, Feng T, Wang C, Liu S,Cheng Q, Oliver D E,Wang X and Xu G *2016 IEEE Sensors Journal* **16** (23) 8381-88
[5] Payne B P, Venugopalan V, Mikić B B and Nishioka N S2003 *Journal of Biomedical Optics* **8** (2) 273-80
[6] Nuster R, Holotta M, Kremser K, Grossauer H, Burgholzer P and Paltauf 2010 *Journal of Biomedical Optics* **15** (2) 021307
[7] Speirs R W and Bishop A I 2013 *Applied Phisics Letters* **103** 053501
[8] Rembe C, Siegmund G, Steger H and Wörtge 2006 Measuring MEMS in motion by Laser Doppler Vibrometry *Optical Inspection of Microsystem* , ed Osten W (Boca Raton: CRC Press)
[9] Esenaliev R O, Karabutov A A,Tittel F K, Fornage B D, Thomsen S L, Stelling C and Oraevsky A A 1997 *Proc. of SPIE - The International Society for Optical Engineering* **2979** 71-82
[10] Oraevsky A A, Andreev V A, Karabutov A A and Esenaliev R O 1999 *Proc. of SPIE - The International Society for Optical Engineering* **3601** 256-67
[11] Oraevsky A A and Karabutov A A 2000 *Proc. of SPIE - The International Society for Optical Engineering* **3916** 228-39
[12] Winkler A M, Maslov K and Wang L V 2013 Noise Equivalent sensitivity of photoacoustics *J. of Biomedical Optics* **18** (9) 097003
[13] Rousseau G, Blouin A and Monchalin J P 2012 *Biomed Optics Express* **3** (1) 16-25
[14] Oraevsky AA and Karabutov A A 2003 Optoacoustic *Tomography Biomedical Photonics Handbook* ed Vo-Dinh T (Boca Raton: CRC Press) Chapter 34, pp. 34/1-34/34.
[15] American National Standard for Safe use of Lasers. Laser Institue of America, Amer. Nat. Standards Institute, Inc; 2007. ANSI Standards Institute, Inc; 2007. ANSI Standard Z136.1-2007